

Annual Modulation Signature for the Direct Detection of Milky Way wimps and Supergravity Models

R. Arnowitt^a and Pran Nath^b

a Center for Theoretical Physics, Texas A & M University,

College Station, TX 77843, USA

b Department of Physics, Northeastern University, Boston, MA 02115, USA

Abstract

An analysis is given of the annual modulation signal for the direct detection of relic neutralinos within the framework of supergravity unified models. It is shown that both the minimal and the non-minimal SUGRA models can generate neutralino-proton cross-sections at the level compatible with the signals reported in the DAMA experiment at the Gran Sasso National Laboratory. Effects of proton stability on the analysis of the DAMA data in the minimal and the non-minimal SUGRA models are also discussed.

1. INTRODUCTION

Last year, the DAMA experiment examined the possibility of the direct detection of Milky Way wimps using the annual modulation signal. Based on a set up of approximately 100 kg of radiopure $NaI(Tl)$ detectors in the Gran Sasso National Laboratory and 4549 kg-day of data, they found an indication of such a signal¹. More recently, an additional 14,962 kg-day of data has significantly strengthened the statistical analysis favoring the presence of a yearly modulation signal² with a wimp mass and proton cross section of

$$M_w = (59_{-14}^{+17}) GeV; \quad \xi \sigma_{w-p} = (7.0_{-1.2}^{+0.4}) \times 10^{-6} pb \quad (1)$$

where $\xi = \rho_w/\rho_0$, ρ_w is the local Milky Way wimp mass density and $\rho_0 = 0.3 \text{ GeVcm}^{-3}$.

In the following, we will analyze the possible consequences of such a signal within the framework of supergravity grand unification models with R-parity invariance and gravity mediated supersymmetry (SUSY) breaking^{3,4}. Such models automatically predict the existence of cold dark matter (CDM) in the universe, i.e. the relic lightest supersymmetric particle (LSP) remaining from the Big Bang. Further, over most of the SUSY parameter space, the LSP is the lightest neutralino, $\tilde{\chi}_1^0$, and the calculated relic density of $\tilde{\chi}_1^0$ is in accord with astronomical estimates over a significant part of the parameter space. For the relic density, we will assume the range $0.05 \leq \Omega_{\tilde{\chi}_1^0} h^2 \leq 0.30$, where $\Omega_{\tilde{\chi}_1^0} = \rho_{\tilde{\chi}_1^0}/\rho_c$, where $\rho_{\tilde{\chi}_1^0}$ is the mean relic density in the universe, $\rho_c = 3H^2/8\pi G_N$, $G_N =$ Newton's constant, and the Hubble constant H is parameterized by $H = (100 \text{ kmsec}^{-1} \text{ Mpc}^{-1})h$.

The annual modulation effect arises due to the motion of the Earth around the Sun. Thus, v_E , the velocity of the Earth relative to the Galaxy is $v_E = v_S + v_0 \cos \gamma \cos \omega(t - t_0)$ where v_S is the Sun's velocity relative to the Galaxy ($v_S = 232 \text{ km/s}$), v_0 is the Earth's orbital velocity around the Sun ($v_0 = 30 \text{ km/s}$) and γ is the angle of inclination of the plane of the Earth's orbit relative to the galactic plane ($\gamma \cong 60^\circ$). One has $\omega = 2\pi/T$ ($T = 1$ year) and the maximum velocity occurs at day $t_0 = 155.2$ (June 2). The change in the Earth's velocity relative to the incident wimps leads to a yearly modulation of the scattering event rates of about 7%.

The calculation of the $\tilde{\chi}_1^0 - p$ cross section proceeds as follows⁵. One first calculates the relic density of $\tilde{\chi}_1^0$, limiting the SUSY parameter space so that the above constraints on $\Omega_{\tilde{\chi}_1^0} h^2$ are obeyed. Within this constrained parameter space, we then calculate the $\tilde{\chi}_1^0 - p$ cross section for incident halo $\tilde{\chi}_1^0$ on the terrestrial target. In comparing the theoretical $\sigma_{\tilde{\chi}_1^0 - p}$ with the data, a number of uncertainties arise due mainly to the lack of knowledge of input parameters. We estimate an error of a factor of 2-3 in these calculations. In addition, $\rho_{\tilde{\chi}_1^0}$ may vary from about $(0.2 - 0.7) \text{ GeVcm}^{-3}$ (i.e., $0.7 \lesssim \xi \lesssim 2.3$).

Supergravity models have a wide range of applicability. Thus, once one phenomena begins to fix the SUSY parameters, it effects predictions in other areas. We will examine

here the effects the DAMA data has on SUSY mass spectrum predictions at future accelerator searches. In addition, most supergravity models predict the existence of proton decay. While the predictions for proton decay are more model dependent than other parts of the theory, there is a strong correlation in the SUSY parameter space between DM detector event rates and the expected proton lifetime⁶, and we will discuss this below.

2. SUPERGRAVITY MODELS

We consider supergravity (SUGRA) models where supersymmetry is broken in a hidden sector at the Planck scale ($M_P = 2.4 \times 10^{18} GeV$) by supergravity interactions and transmitted to the physical sector by supergravity, giving rise to soft breaking terms³. If the hidden sector interactions are generation independent, one obtains the simplest model, mSUGRA, with universal soft breaking parameters at the GUT scale $M_G \simeq 2 \times 10^{16} GeV$. The renormalization group equations (RGE) then show that the SUSY soft breaking at M_G generates $SU(2) \times U(1)$ breaking at the electroweak scale. This model then depends on four parameters and one sign (in addition to the parameters of the SM). One can choose these parameters to be the following: m_0 , the universal scalar soft breaking mass at M_G ; $m_{1/2}$, the universal gaugino mass at M_G (or alternately the gluino mass $m_{\tilde{g}} \cong (\alpha_3(M_Z)/\alpha_G)m_{1/2}$ where $\alpha_G \cong 1/24$ is the coupling constant at M_G); A_0 , the universal cubic soft breaking parameter (or alternately A_t , the t-quark parameter at the electroweak scale); and $\tan\beta = \langle H_2 \rangle / \langle H_1 \rangle$ where $\langle H_2 \rangle$ gives rise to the up quark masses and $\langle H_1 \rangle$ to the down quark and the lepton masses. The RGE then determines μ^2 (where μ is the Higgs mixing parameter in the superpotential term $\mu H_1 H_2$), leaving the sign of μ arbitrary.

The mSUGRA model contains relatively few new parameters, and existing data has begun to limit this parameter space. Thus, the measured value of the t-quark mass and the $b \rightarrow s + \gamma$ branching ratio eliminate most of the $\mu < 0$ and $A_t < 0$ part of the parameter space⁷. However, the supergravity formalism allows for non-universal soft breaking⁸. While the universality of the soft breaking mass m_0 guarantees the suppression of flavor changing

neutral currents (FCNC), the FCNC are not sensitive to the Higgs mass or to the third generation non-universalities and string models can allow for such non-universality. We parameterize this possibility by the following Higgs soft breaking masses at M_G ,

$$m_{H_1}^2 = m_0^2(1 + \delta_1); \quad m_{H_2}^2 = m_0^2(1 + \delta_2) \quad (2)$$

and the following third generation sfermion masses:

$$m_{q_L}^2 = m_0^2(1 + \delta_3); \quad m_{u_R}^2 = m_0^2(1 + \delta_4); \quad m_{e_R}^2 = m_0^2(1 + \delta_5)$$

$$m_{d_R}^2 = m_0^2(1 + \delta_6); \quad m_{\ell_L}^2 = m_0^2(1 + \delta_7) \quad (3)$$

where $q_L = (t_L, b_L)$, $u_R = t_R$, $\ell_L = (\nu_L, e_L)$, etc. m_0 is the universal soft breaking mass of the first two generations, and δ_i represents the non-universal deviations. For soft breaking occurring above M_G , and for GUT groups having an $SU(5)$ subgroup (e.g. $SU(N)$, $N \geq 5$, $SO(N)$, $N \geq 10$, E_6 , etc.) with matter embedded into 10 and $\bar{5}$ representations in the usual way, one has $\delta_3 = \delta_4 = \delta_5$ and $\delta_6 = \delta_7$. We assume in the following that $|\delta_i| \leq 1$.

The non-universal corrections enter sensitively in μ^2 . For $\tan \beta \leq 25$, δ_5, δ_6 and δ_7 make only small contributions, and a closed form expression can be obtained for μ^2 at the electroweak scale⁹

$$\mu^2 = \frac{t^2}{t^2 - 1} \left[\left(\frac{1 - 3D_0}{2} + \frac{1}{t^2} \right) + \left(\frac{1 - D_0}{2} (\delta_3 + \delta_4) - \frac{1 + D_0}{2} \delta_2 + \frac{1}{t^2} \delta_1 \right) \right] m_0^2$$

$$+ \frac{t^2}{t^2 - 1} \left[\frac{1}{2} (1 - D_0) \frac{A_R^2}{D_0} + C_\mu m_{1/2}^2 \right] - \frac{1}{2} M_Z^2 + \frac{1}{22} \frac{t^2 + 1}{t^2 - 1} S_o \left(1 - \frac{\alpha_1(Q)}{\alpha_G} \right) + 1 \text{ loop terms} \quad (4)$$

where $t \equiv \tan \beta$, $C_\mu = \frac{1}{2} D_0 (1 - D_0) (H_3/F)^2 + e - g/t^2$, and $D_0 \simeq 1 - m_t^2 / (200 \sin \beta)^2$. D_0 vanishes at the t-quark Landau pole (for $m_t = 175 \text{ GeV}$, $D_0 \leq 0.23$) and $A_R = A_t - m_{1/2} (H_2 - H_3/F)$ is the residue at the Landau pole ($A_R \cong A_t - 0.61 (\alpha_3/\alpha_G) m_{1/2}$), i.e. $A_0 = A_R/D_0 - (H_3/F) m_{1/2}$. $S_o = \text{Tr} Y m^2$ where Y is the hypercharge and m^2 are the squark and Higgs masses at M_G of Eqs. (2,3). The form factors H_2, H_3, F, e, g are given in Ref.¹⁰.

μ^2 enters importantly in the theoretical predictions of dark matter event rates. Thus, if μ^2 is reduced, the predicted rates generally increase, and if μ^2 is increased, they go down. From Eq.(4), we see that the non-universal parameters thus can play an important role, as for one set of signs (i.e., $\delta_{1,3,4} < 0$, $\delta_2 > 0$) μ^2 will be reduced, and the opposite set will increase μ^2 .

3. COMPARISON WITH DAMA DATA

We compare in this section, the DAMA data with the theoretical expectations for SUGRA models. The analysis is carried out using the constraints arising from the radiative breaking of the electro-weak symmetry and the accurate method for the computation of the relic density¹¹.

(i) mSUGRA model

In this model, all the δ_i are set to zero, and the theory is very restricted. Fig. 1 shows the experimental bound of the DAMA data for $\sigma_{\chi_1^0-p}$ (dotted lines) vs. $m_{\chi_1^0}$ for the spin independent $\chi_1^0 - p$ cross section, where we have combined the 95%*CL* bound of DAMA with the uncertainty in the Milky Way density $\rho_{\tilde{\chi}_1^0}$ ($0.7 \leq \xi \leq 2.3$). (The *NaI* detector is sensitive only to the spin independent interaction.) The solid curves are the maximum and minimum theoretical cross section $\sigma_{\chi_1^0-p}$ for $\tan\beta \leq 30$ (as one scans over the allowed part of the parameter space). In general, the maximum cross section occurs for the maximum values of $\tan\beta$, so that the upper solid curve occurs for $\tan\beta = 30$. The dashed curve corresponds to $\tan\beta = 20$ and the dot-dash curve to $\tan\beta = 10$.

The general behavior of the theoretical curves follow from an interplay between the $\tilde{\chi}_1^0$ early universe annihilation cross section (leading to current relic density) and the $\tilde{\chi}_1^0$ - quark cross section in the terrestrial DM detector¹². In the relic density analysis, there are two regions in the neutralino annihilation cross section. For $m_{\chi_1^0} \lesssim 50 - 60$, annihilation can occur rapidly through s-channel Z and *h* poles, allowing (and sometimes requiring) m_0 to be large (e.g., $m_0 = (500 - 1000)GeV$) so that the lower bound, $\Omega_{\chi_1^0} h^2 > 0.05$, not be violated.

For $m_{\tilde{\chi}_1^0} \gtrsim 50 - 60 \text{ GeV}$, the t-channel annihilation through sfermion poles dominates (as one now has $2m_{\tilde{\chi}_1^0} > m_h, M_Z$) and one requires m_0 to be small (e.g., $m_0 \lesssim 150 \text{ GeV}$) in order that the sfermions are sufficiently light so that there is sufficient annihilation to ensure that the upper bound $\Omega_{\tilde{\chi}_1^0} h^2 < 0.3$ not be violated. Thus as $m_{\tilde{\chi}_1^0}$ is increased past 50 GeV, m_0 decreases. In contrast, the detector $\tilde{\chi}_1^0$ -quark cross section has a major contribution from the s-channel squark pole and so increases as m_0 is reduced. In addition, this cross section falls off with increasing neutralino mass.

The above effects can be seen in Fig. 1. The $\sigma_{\tilde{\chi}_1^0-p}$ cross section rises as $m_{\tilde{\chi}_1^0}$ increases and subsequently falls off with increasing $m_{\tilde{\chi}_1^0}$. This leads to a maximum theoretical cross section at $m_{\tilde{\chi}_1^0} \simeq 55 \text{ GeV}$, which fortuitously is in the region where the DAMA detector is most sensitive. One can therefore accommodate the DAMA data for $\tan\beta > 8$.

(ii) Models with Non-universal Soft Breaking Non-universal soft breaking can significantly effect the analysis, since as discussed above, μ^2 of Eq.(4) can be decreased or increased depending on the signs of the δ_i . Thus for the cases where $\delta_1, \delta_2, \delta_3 < 0$ and $\delta_4 > 0$ one finds that μ^2 decreases, and a smaller μ^2 tends to enhance the event rates and the $\tilde{\chi}_1^0 - p$ cross-section. We study this case in Fig.2 where we consider $\delta_1 = -1 = -\delta_2$ and $\delta_3 = -1 = \delta_4$. Here we find that for $\tan\beta \leq 30$ theoretical predictions often exceed the upper limit of the 2σ corridor of DAMA whereas for the mSUGRA case the upper limit of theoretical predictions lie within the DAMA corridor (see Fig.1). Similarly the theoretical predictions for the case $\tan\beta \leq 10$ lie significantly higher than the corresponding predictions for the mSUGRA case. Infact in this case one can achieve consistency with DAMA for values of $\tan\beta$ as low as 6. Further the allowed $\tilde{\chi}_1^0$ mass range consistent with the DAMA modulation signal extends over a somewhat larger domain of $\tan\beta$ relative to the mSUGRA case as may be seen by comparison of Fig.1 and Fig.2.

4. CONSTRAINTS OF PROTON DECAY

Many SUGRA models which possess a neutralino dark matter candidate, also give rise to proton decay. While predictions of proton decay are more model dependent than in other phenomena, it has been observed that cosmological constraints strongly affect predictions for the proton lifetime τ_p , and correspondingly, experimental bounds on τ_p affect expected DM detector rates⁶.

We consider here GUT groups which contain an SU(5) subgroup with matter embedded into the 10 and $\bar{5}$ of SU(5) in the usual way. For these models, proton decay proceeds mainly through the mode $p \rightarrow \bar{\nu} + K^+$, with a u and d quark converted into \tilde{d}_i and \tilde{u}_i squarks (i = generation index) by a t-channel chargino (χ_j^\pm), and the squarks are then converted into a $\bar{\nu}$ and a \bar{s} -quark by the B and L violating interactions of the superheavy color triplet Higgsinos, \tilde{H}_3 and $\tilde{\bar{H}}_3$ ^{13,14}. The proton lifetime is then

$$\tau_p^{-1} = \Gamma(p \rightarrow \bar{\nu}K) = \sum_{i=e,\mu,\tau} \Gamma(p \rightarrow \bar{\nu}_i K^+) \quad (5)$$

In general, the second generation dominates and in order to get the maximum lifetime, τ_{max} , we assume that the third generation, which enters with arbitrary phase and is about a 20% effect, interferes destructively with the second generation. We will also limit the \tilde{H}_3 mass to obey $M_{H_3} \leq 10 M_G$, as larger values of M_{H_3} would be in the domain of strong gravitational effects not being considered in SUGRA models.

The current Super Kamiokande bound on τ_p for the $p \rightarrow \bar{\nu}K$ mode is¹⁵

$$\tau_p(p \rightarrow \bar{\nu}K) > 5.5 \times 10^{32} \text{ yr}; \quad 90\% \text{ C.L.} \quad (6)$$

One may obtain a qualitative picture of the dependence of τ_p on the SUSY parameters by noting that the dominant second generation contribution is roughly scaled by¹⁴

$$\Gamma(p \rightarrow \bar{\nu}K) \sim \frac{1}{M_{H_3}^2} \left(\frac{m_{\chi_1^0} \tan \beta}{m_{\tilde{q}}^2} \right)^2 \quad (7)$$

Thus large $m_{\chi_1^0}$ (i.e. large $m_{\tilde{q}}$), small $m_{\tilde{q}}$ and large $\tan \beta$ will destabilize the proton. This puts strong constraints on the allowed region of the parameter space when combined with

the relic density constraint $0.05 \leq \Omega_{\tilde{\chi}_1^0} h^2 \leq 0.30$. The DAMA data puts additional strong constraints on the mSUGRA models.

In more general situations the Higgs triplet sector of the theory can be more complicated and one can have many Higgs triplets which mediate p decay. Thus as discussed in ref.¹⁶ in the presence of many Higgs triplets one has a Higgs triplet mass term $\bar{H}_i M_{ij} H_j$, and one can make a redefinition of fields so that only the Higgs triplet \bar{H}_1 and H_1 couple to matter. The Higgs triplet couplings to matter then are of the form $\bar{H}_1 J + \bar{K} H_1$, where J and \bar{K} are bilinear in matter (i.e., quark and lepton fields). If one integrates out the Higgs triplet fields, the resulting baryon and lepton number violating dimension five operator is given by¹⁶ $W_4 = -\bar{K}(M^{-1})_{11} J$. Thus for a 2×2 matrix M , a suppression by a factor of ≈ 3 (e.g., by the choice $M_{11} = -2M_{22} = M$, $M_{12} = M_{21} = M$) in the proton decay amplitude and a suppression by a factor of ≈ 10 in the proton decay rate is easily obtained. In this case the proton lifetime can be significantly enhanced.

We discuss now the numerical analysis of $\sigma_{\tilde{\chi}_1^0-p}$ with the inclusion of the proton lifetime constraint. It turns out that with the imposition of the proton lifetime limits, one finds no points in the parameter space consistent with DAMA data for the minimal SU(5) case. However, a non-trivial region of the parameter space does exist for non-minimal SUGRA models where one can get consistency simultaneously with both the DAMA data on annual modulation and the proton lifetime limits. The non-minimalities can arise in various forms. We have already discussed non-minimalities in the soft SUSY breaking parameters where non-minimality implies going beyond mSUGRA to include non-universal soft breaking. However, since proton decay involves GUT physics one finds that there are other non-minimalities needed to generate acceptable physics at low energy. Thus the minimal SU(5) model does not lead to satisfactory quark and lepton mass matrices. One may modify it, however, to generate, e.g. the Georgi-Jarlskog texture at M_G , leading to reasonably correct quark and lepton masses. This requires additional GUT interactions which give rise to an increase in τ_p of about a factor of 3-5¹⁷. In addition to this, there are other theoretical uncertainties in the calculation of τ_p , relating to input parameters, e.g. the three quark

matrix element of the proton¹⁸, and we estimate an additional uncertainty of a factor of 2-3. Thus a factor of 10 enhancement is possible for the p lifetime from these factors. Further the structure of GUT physics is of course largely unknown. In general as discussed above one can conceive of multi Higgs triplets which participate in mediating p decay. As discussed above a factor of ten enhancement in the proton lifetime can occur from this source without significant fine tuning. Including the enhancements discussed from effects of textures etc. one can generate a total enhancement of a factor of $\sim 10^2$.

An analysis of $\chi_1^0 - p$ cross sections with proton decay constraints including the above enhancement factors is given in Fig.3 for the case of universal soft SUSY breaking parameters. One finds that there is a small region of the parameter space where both the DAMA and the proton lifetime constraints are satisfied. The allowed $\tilde{\chi}_1^0$ mass region is close to the peak of the DAMA experiment. Next we carry out the analysis for models with non-universal soft SUSY breaking. The model which is favorable for both DAMA and proton stability is given in Fig.4. It corresponds to the case $\delta_1 = -0.5 = -\delta_2$. The analysis shows that with enhancement factors as discussed above one can achieve consistency with DAMA and proton lifetime limit over a broad range of $\tilde{\chi}_1^0$ mass and within the range given by DAMA. This model produces an interesting range of mass spectra for the SUSY particles. Two of the supersymmetric particles which are likely candidates for discovery at colliders are the Higgs and the lightest chargino. We exhibit the scatter plot of their masses in this model in Fig.5. Their mass ranges are such that they should be accessible at TeV(33).

5. CONCLUSION

In this paper we have given an analysis of the annual modulation signal observed by DAMA for the direct detection of dark matter within the framework of supergravity models¹⁹. We find that SUGRA models with and without non-universalities can easily accommodate the range of $\tilde{\chi}_1^0 - p$ cross-sections needed to explain the observed signal. However, in SUGRA models with grand unification, proton lifetime limits impose additional constraints. Thus for

the case of the minimal SU(5) mSUGRA model it appears not possible to explain the DAMA signal and simultaneously satisfy the current proton lifetime lower limits. However, SUGRA models with textures and with more complex Higgs triplet structure can allow one to significantly enhance the p decay lifetime. Similarly, SUGRA models with non-universalities also affect the proton lifetime as well as $\tilde{\chi}_1^0 - p$ cross-section. It is shown that within the context of these non-minimal SUGRA models one can achieve consistency with the signal and a satisfaction of the proton lifetime limits. The sparticle mass spectra is also investigated. It is shown that the lightest particles in this model are the neutralino $\tilde{\chi}_1^0$, the light chargino $\tilde{\chi}_1^\pm$, and the light Higgs h^0 which should all be accessible at the TeV(33) and the LHC.

Acknowledgements

This research was supported in part by NSF grant PHY-9722090 and PHY-96020274.

Figure Captions

Fig1. Plot of the maximum and minimum of $\tilde{\chi}_1^0 - p$ cross-section vs neutralino mass for mSUGRA for various ranges of tanbeta when other parameters are allowed to vary over the ranges $m_0, m_{\tilde{g}} \leq 1TeV$ and A_0 is allowed to vary over the range consistent with electro-weak symmetry breaking. The various cases correspond to $\tan\beta \leq 30$ (solid), $\tan\beta \leq 20$ (dashed), and $\tan\beta \leq 10$ (dot-dashed). The minimum dashed and dot-dashed curves overlap the minimum solid curve. The dotted curves give the experimental 95%CL range implied by the DAMA annual modulation data combined with the uncertainty in ξ .

Fig2. Plot of the maximum and minimum of $\tilde{\chi}_1^0 - p$ cross-section vs neutralino mass for the non-universal SUGRA model with $\delta_1 = -1 = -\delta_2$, $\delta_3 = -1 = \delta_4$ for various ranges of $\tan\beta$ when other parameters are allowed to vary over the ranges $m_0, m_{\tilde{g}} \leq 1TeV$ and A_0 is allowed to vary over the range consistent with electro-weak symmetry breaking. The various cases correspond to $\tan\beta \leq 30$ (solid), $\tan\beta \leq 10$ (dashed), and $\tan\beta \leq 8$ (dot-dashed). The minimum dashed and dot-dashed curves overlap the minimum solid curve over most of the neutralino mass range. The horizontal curves are as in Fig.1.

Fig3. Plot of the maximum and minimum of $\tilde{\chi}_1^0 - p$ cross-section vs neutralino mass for mSUGRA exhibiting the proton lifetime constraint. The maximum and minimum solid curves are for $\tan\beta \leq 30$ as in Fig.1. The region enclosed by the long dashed curve and the minimum solid line is the region allowed under the proton life time constraint with an enhancement factor of 10^2 as discussed in the text. The region enclosed by the dot-dashed lines on the left and the region enclosed by the dot-dashed line and the minimum solid line to the right is the region allowed with proton life time constraint with an enhancement factor of 20.

Fig4. Plot of the maximum and minimum of $\tilde{\chi}_1^0 - p$ cross-section vs neutralino mass for the non-universal SUGRA model with $\delta_1 = -0.5 = -\delta_2$, and $\delta_3 = 0 = \delta_4$ exhibiting the proton lifetime constraint. The maximum and minimum solid curves are for the case when $\tan\beta \leq 30$ but without imposition of proton lifetime constraint. The region enclosed by the long dashed curve and the minimum solid line is the region allowed by the proton lifetime constraint with an enhancement factor of 10^2 . The region enclosed by the dot-dashed lines is the region allowed by the proton life time constraint with an enhancement factor of 20.

Fig5. The scatter plot of light chargino mass \tilde{W}_1 (filled squares) and the light Higgs h^0 (open circles) for the case $\delta_1 = -0.5 = -\delta_2$ for the set of points that satisfy the DAMA range as shown in Fig.1 and the proton stability constraint corresponding to the area enclosed by the dashed curves in Fig4.

REFERENCES

1. R. Bernabei et al, Phys. Lett. B424, 195(1998).
2. R. Bernabei et al, INFN/AE-98/34, (1998).
3. A.H. Chamseddine, R. Arnowitt, and P. Nath, Phys. Rev. Lett. **49**, 970(1982).
4. For a review see, P. Nath, R. Arnowitt and A.H. Chamseddine, Applied N=1 supergravity, Trieste Lectures, 1983(World Scientific, Singapore); H. P. Nilles, Phys. Rep. **110**, 1(1984); H.E. Haber, G.L.Kane. Phys.Rep. **117**, 195(1984); R. Arnowitt and P. Nath, Proc. of VII J.A. Swieca Summer School, ed. E. Eболи (World Scientific, Singapore, 1994).
5. For a review see, G. Jungman, M. Kamionkowski, and K. Griest, Phys. Rep. **267**, (1995)195.
6. R. Arnowitt and P. Nath, Phys. Lett. **B437**, 344(1998).
7. P. Nath and R. Arnowitt, Phys. Lett. **B336**, 395(1994); F. Borzumati, M. Drees, and M.M. Nojiri, Phys. Rev.**D51**, 341(1995); V. Barger and C. Kao, Phys. Rev. bf D57, 3131(1998); H. Baer, M. Brhlik, D. Castano and X. Tata, Phys. Rev. **D58**, 015007(1998).
8. S.K.Soni and H.A. Weldon, Phys.Lett.**B126**,215(1983); V.S.Kaplunovsky and J.Louis, Phys.Lett.**B306**, 268(1993); D.Matalliotakis and H.P.Nilles, Nucl.Phys.**B435**, 115(1995); M.Olechowski and S.Pokorski, Phys.Lett. **B344**, 201(1995); N.Polonsky and A.Pomerol, Phys.Rev.**D51**, 6532(1995); V.Berezinsky et al, CERN-TH 95-206; R. Arnowitt and P. Nath, Phys. Rev. **D56**, 4194(1997).
9. P. Nath and R. Arnowitt, Phys. Rev. **D56**, 2820(1997).
10. L. Ibanez, C. Lopez, and C. Munos, Nucl. Phys. **B256**, 218(1985).
11. K. Greist and D. Seckel, Phys. Rev. **D43**, 3191 (1991); P. Gondolo and G. Gelmini, Nucl.

- Phys. **B360**, 145 (1991); R. Arnowitt and P. Nath, Phys. Lett. **B299**, 103(1993); Phys. Rev. Lett. **70**, 3696(1993); Phys. Rev. **D54**, 2374(1996); M. Drees and A. Yamada, Phys. Rev. **D53**, 1586(1996); H. Baer and M. Brhlik, Phys. Rev. **D53**, 597(1996); V. Barger and C. Kao, Phys. Rev. **D57**, 3131(1998).
12. E. Ellis and R. Flores, Phys. Lett. **B300**, (1993)175; M. Drees, M. Nojiri, Phys. Rev. **D48**, (1993)3483; V. Bednyakov, H.V. Klapdor-Kleingrothaus and S. Kovalenko, Phys. Rev. **D50**, (1994)7128; A. Bottino et.al., Astropart. Phys. **2**, (1994)77; R. Arnowitt and P. Nath, Mod. Phys. Lett. **A 10**,1257(1995); Phys. Rev.**D54**,2374(1996). P. Nath and R. Arnowitt, Phys. Rev. Lett. **74**, (1995)4592 ; E. Diehl, G. Kane, C. Kolda and J. Wells, Phys. Rev. **D52**, (1995)4223; L. Bergstrom and P. Gondolo, Astropart. Phys. **5**, (1996)263; H. Baer and M. Brhlik, Phys. Rev. **D57**, (1998)567.
 13. S. Weinberg, Phys. Rev. **D26**, 287 (1982); N. Sakai and T. Yanagida, Nucl. Phys.**B197**, 533 (1982); S. Dimopoulos, S. Raby and F. Wilczek, Phys.Lett. **112B**, 133 (1982); J. Ellis, D.V. Nanopoulos and S. Rudaz, Nucl. Phys. **B202**, 43 (1982).
 14. R. Arnowitt, A.H. Chamseddine and P. Nath, Phys. Lett. **156B**, 215(1985); P. Nath, R. Arnowitt and A.H. Chamseddine, Phys. Rev. **32D**, 2348(1985); J. Hisano, H. Murayama and T. Yanagida, Nucl. Phys. **B402**, 46(1993).
 15. M.Takita, talk at the International Conference on High Energy Physics, Vancouver, July, 1998.
 16. R. Arnowitt and P. Nath, Phys. Rev. **D49**, 1479 (1994).
 17. P. Nath, Phys. Rev. Lett. **76**, 2218(1996).
 18. M.B. Gavela et.al., Nucl. Phys. **B312**, 269(1989).
 19. While this work was in progress there appeared an analysis by Bottino et al., hep-ph/9808459, where the analysis of the new DAMA data in supergravity schemes is carried out. However, in this analysis the constraints of proton stability are not imposed

and non-universal soft breaking in the third generation was not considered.

Fig.1: mSUGRA

DAMA: $0.7 < \xi < 2.3$

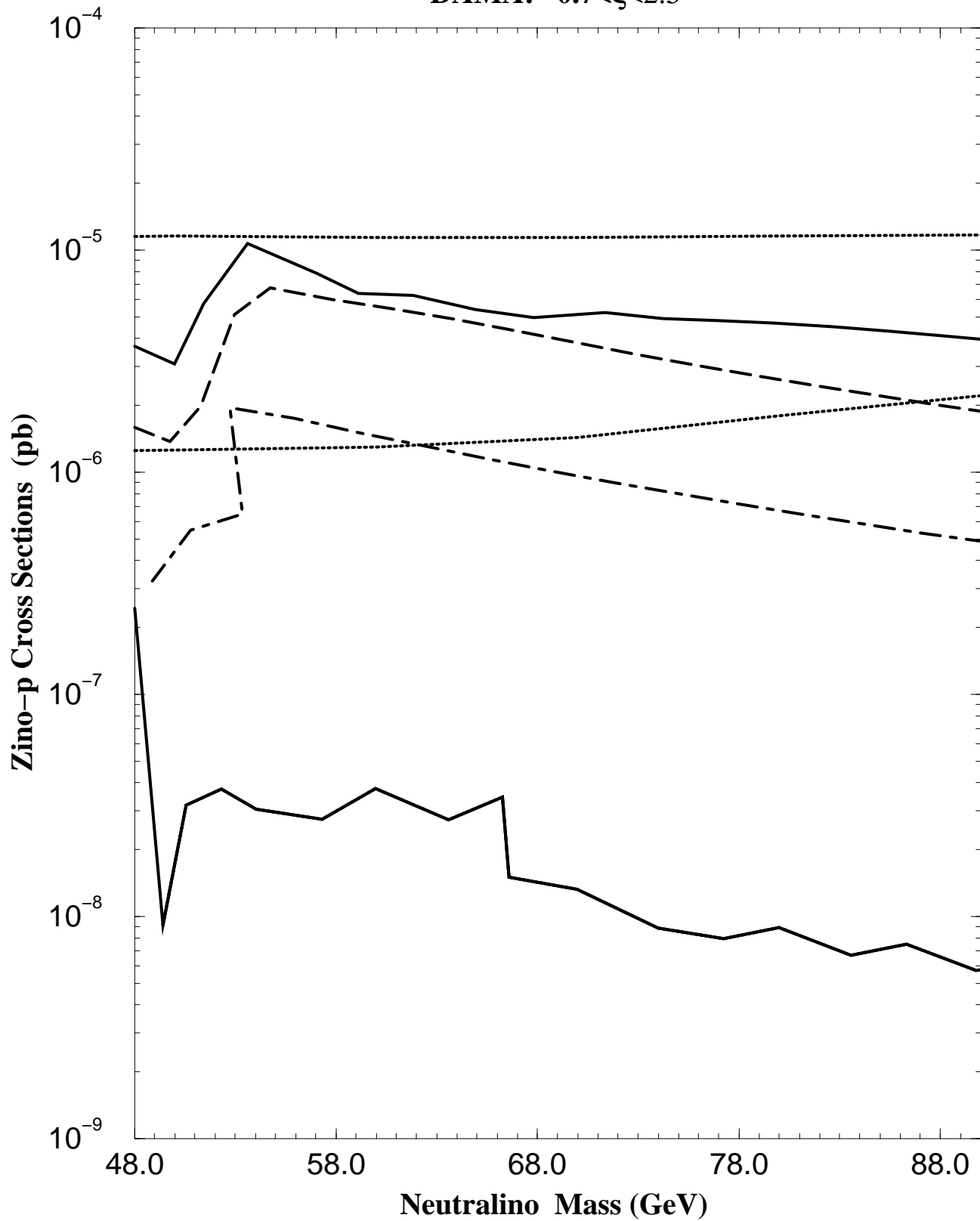


Fig.2: SUGRA $\delta_1=-1=-\delta_2$, $\delta_3=-1=\delta_4$

DAMA: $0.7 < \xi < 2.3$

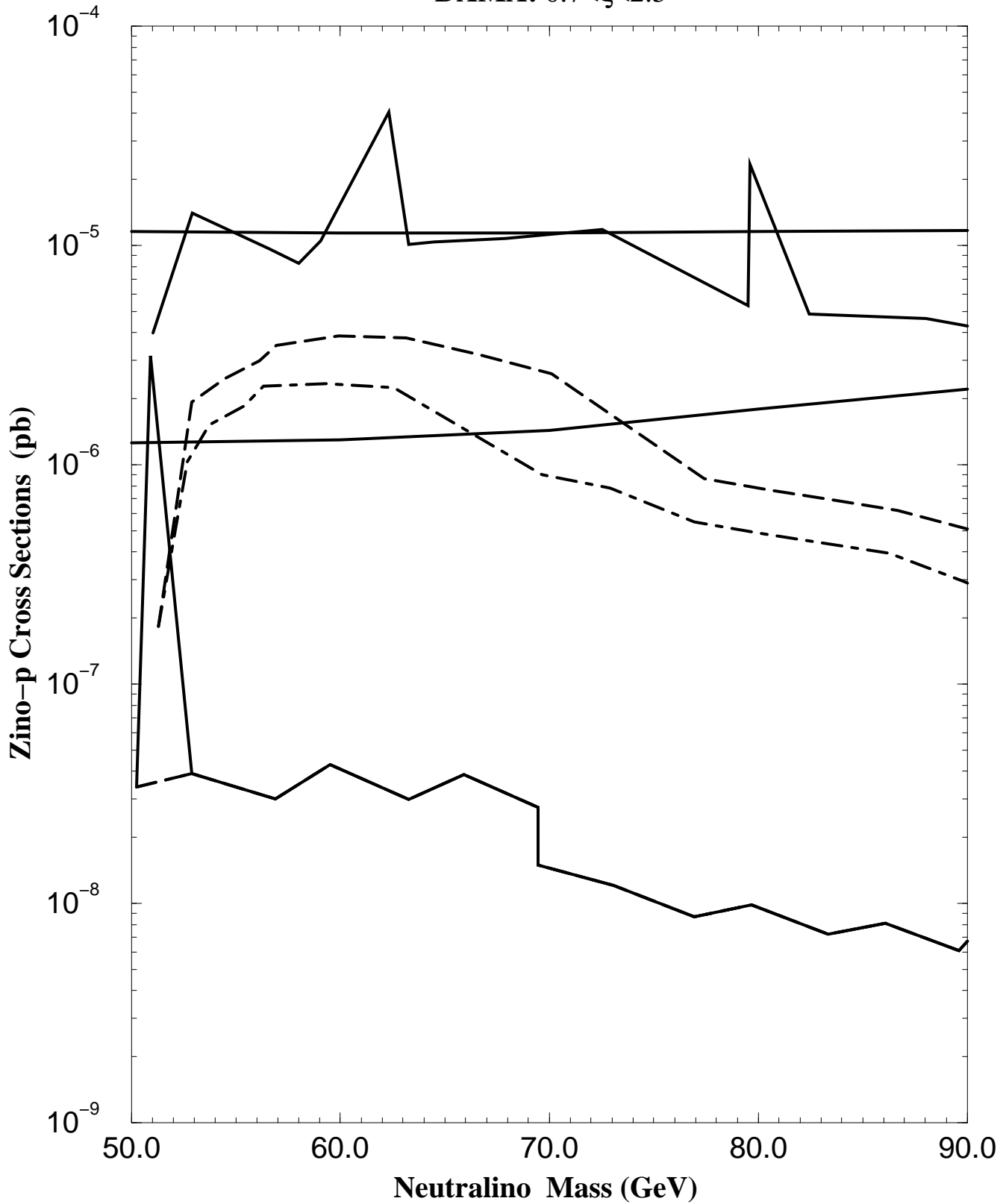


Fig.3

DAMA: $0.7 < \xi < 2.3$

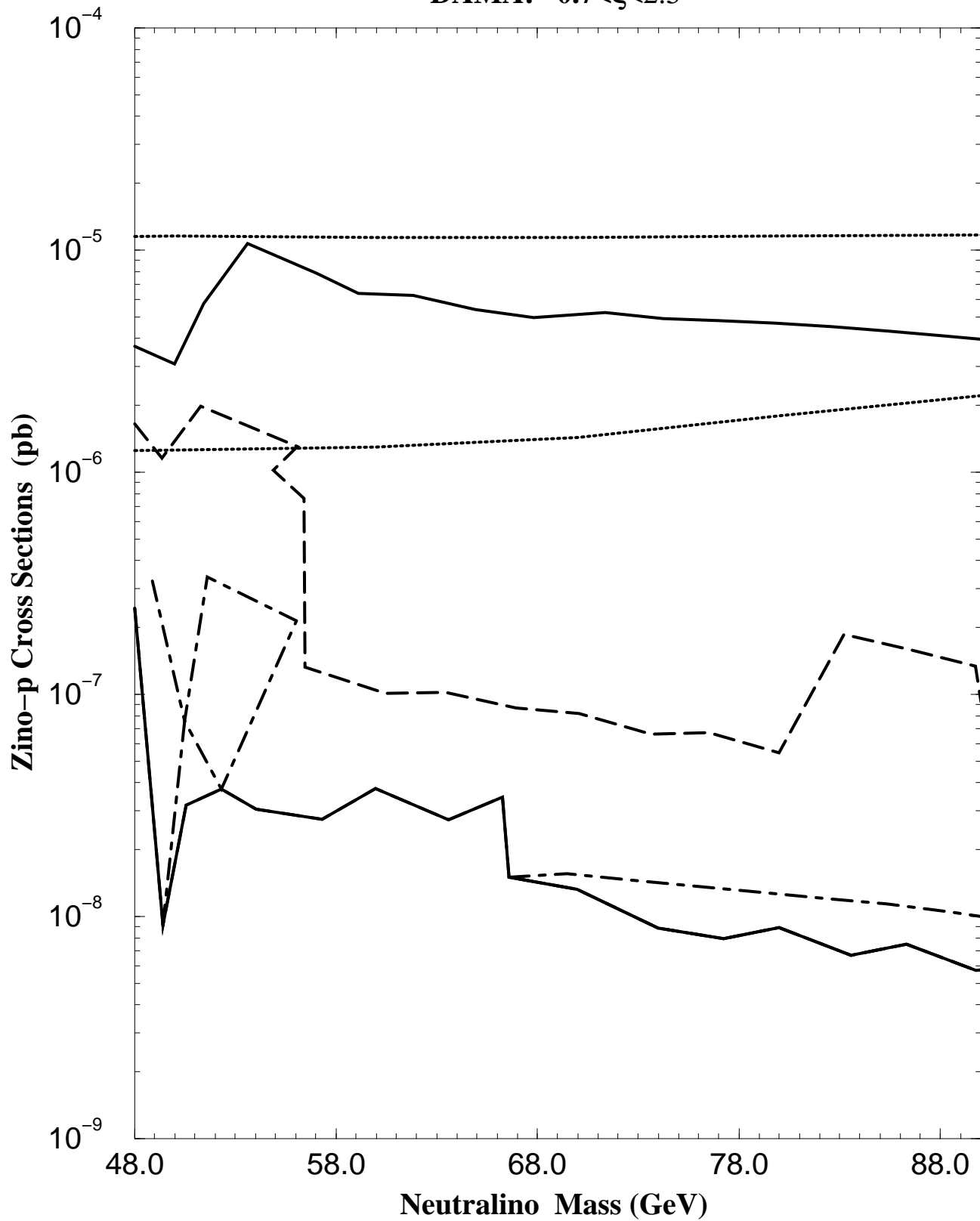


Fig.4: $\delta_1 = -0.5 = -\delta_2$

DAMA: $0.7 < \xi < 2.3$

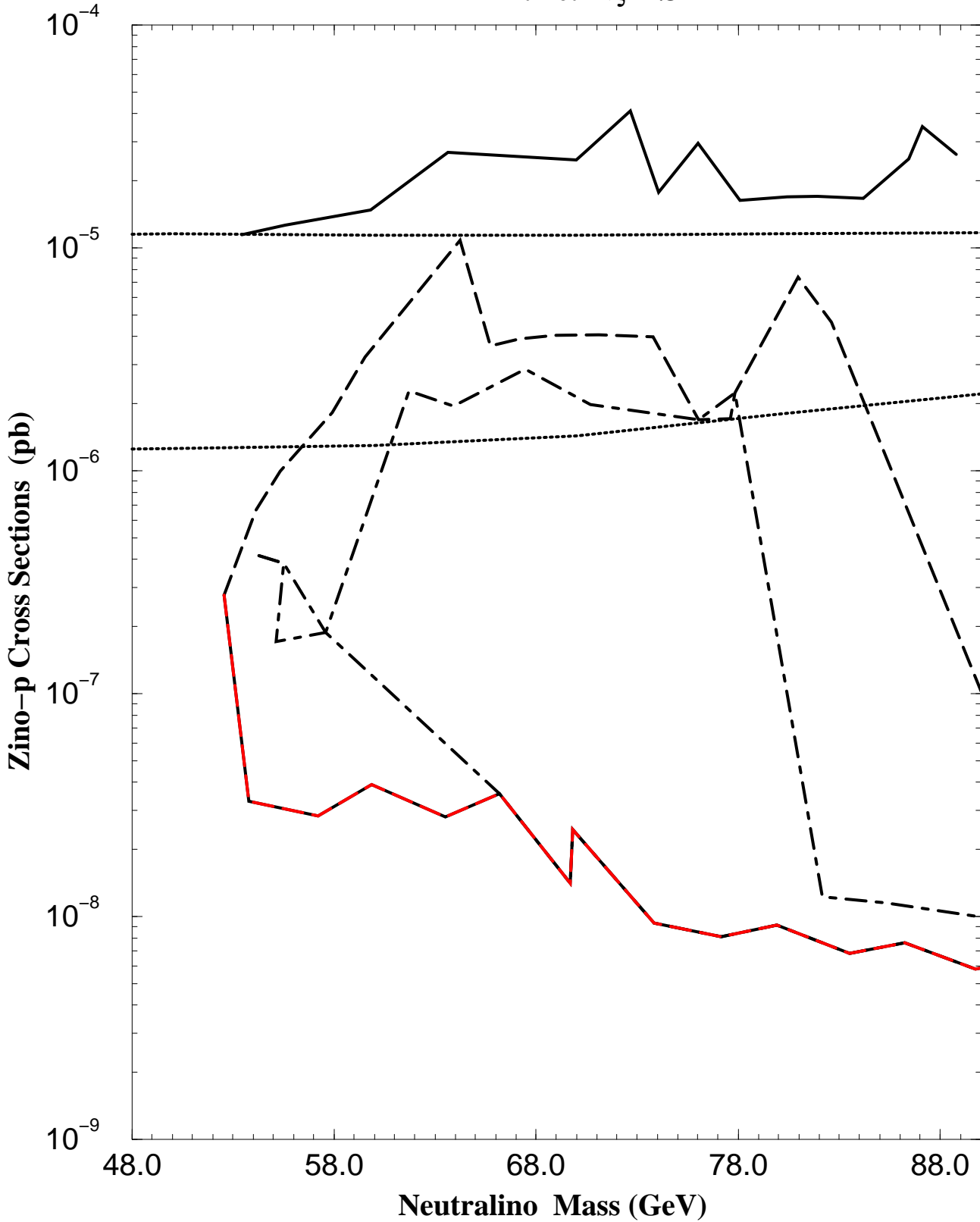


Fig.5

